

1 Large scale genomic analysis of 3067 SARS- 2 CoV-2 genomes reveals a clonal geo-distribution 3 and a rich genetic variations of hotspots 4 mutations

5 Meriem LAAMARTI[¶], Tarek ALOUANE[¶], Souad KARTTI¹, M.W. CHEMAO-
6 ELFIHRI¹, Mohammed HAKMI¹, Abdelounim ESSABBAR¹, Mohamed LAAMART¹,
7 Haitam HLALI¹, Loubna ALLAM¹, Naima EL HAFIDI¹, Rachid EL JAOUDI¹, Imane
8 ALLALI², Nabila MARCHOUDI³, Jamal FEKKAK³, Houda BENRAHMA⁴, Chakib
9 NEJJARI⁵, Saaid AMZAZI², Lahcen BELYAMANI⁶ and Azeddine IBRAHIMI^{1*}

10
11
12
13 ¹ Medical Biotechnology Laboratory (MedBiotech), Bioinova Research Center, Rabat
14 Medical & Pharmacy School, Mohammed Vth University in Rabat, Morocco

15 ² Laboratory of Human Pathologies Biology, Department of Biology, Faculty of Sciences,
16 and Genomic Center of Human Pathologies, Faculty of Medicine and Pharmacy,
17 Mohammed V University in Rabat, Morocco.

18 ³ Anoual Laboratory of Radio-Immuno Analysis, Casablanca, Morocco.

19 ⁴ Faculty of Medicine, Mohammed VI University of Health Sciences (UM6SS),
20 Casablanca, Morocco.

21 ⁵ International School of Public Health, Mohammed VI University of Health Sciences
22 (UM6SS), Casablanca, Morocco.

23 ⁶ Emergency Department, Military Hospital Mohammed V, Rabat Medical & Pharmacy
24 School, Mohammed Vth University in Rabat, Morocco.
25
26

27 * Corresponding author: a.ibrahimi@um5s.net.ma

28 [¶] These authors contributed equally to this work

30

31

32

33 **Abstract**

34 In late December 2019, an emerging viral infection COVID-19 was identified in Wuhan,
35 China, and became a global pandemic. Characterization of the genetic variants of SARS-
36 CoV-2 is crucial in following and evaluating their spread across countries. In this study,
37 we collected and analyzed 3,067 SARS-CoV-2 genomes isolated from 59 countries during
38 the first three months after the onset of this virus. Using comparative genomics analysis,
39 we traced the profiles of the whole-genome mutations and compared the frequency of each
40 mutation in the studied population. The accumulation of mutations during the epidemic
41 period with their geographic locations was also monitored. The results showed 716 site
42 mutations, of which 457 (64%) had a non-synonymous effect. Frequencies of mutated
43 alleles revealed the presence of 39 recurrent non-synonymous mutations, including 10
44 hotspot mutations with a prevalence higher than 0.10 in this population and distributed in
45 six genes of SARS-CoV-2. The distribution of these recurrent mutations on the world map
46 revealed certain genotypes specific to the geographic location. We also found co-occurring
47 mutations resulting in the presence of several haplotypes. Thus, evolution over time has
48 shown a mechanism of co-accumulation and the phylogenetic analysis of this population
49 indicated that this virus can be divided into 3 clades, including a subgroup-specific to the
50 genomes of the United States. On the other hand, analysis of the selective pressure revealed
51 the presence of several negatively selected residues that could be useful for considerations
52 as therapeutic target design.

53 We have also created an inclusive unified database (<http://moroccangenomes.ma/covid/>)
54 that lists all of the genetic variants of the SARS-CoV-2 genomes found in this study with
55 phylogeographic analysis around the world.

56

57 **Keywords:** SARS-CoV-2, Hotspots mutations, Dissemination, Genomic analysis.

58

59

60

61

62

63

64 **Introduction**

65 The recent emergence of the novel, human pathogen Severe Acute Respiratory Syndrome
66 Coronavirus 2 (SARS-CoV-2) in China with its rapid international spread poses a global
67 health emergency. On March 11, 2020, World Health Organization (WHO) publicly
68 announced the SARS-CoV-2 epidemic as a global pandemic. As of March 23, 2020, the
69 COVID-19 pandemic had affected more than 190 countries and territories, with more than
70 464,142 confirmed cases and 21,100 deaths (1).

71 The new SARS-CoV-2 coronavirus is an enveloped positive-sense single-stranded RNA
72 virus (2) and member of a large family named coronavirus which have been classified
73 under three groups (2) two of them are responsible for infections in mammals (2), such us:
74 bat SARS-CoV-like; Middle East respiratory syndrome coronavirus (MERS-CoV). Many
75 recent studies have suggested that SARS-CoV-2 was diverged from bat SARS-CoV-like
76 (3-4).

77 The size of the SARS-CoV2 genome is approximately 30 kb and its genomic structure has
78 followed the characteristics of known genes of Coronavirus; the polyprotein ORF1ab also
79 known as the polyprotein replicase covers more than 2 thirds of the total genome size,
80 structural proteins, including spike protein, membrane protein, envelope protein and
81 nucleocapsid protein. There are also six ORFs (ORF3a, ORF6, ORF7a, ORF7b, ORF8 and
82 ORF10) predicted as hypothetical proteins with no associated function (5).

83 Characterization of viral mutations can provide valuable information for assessing the
84 mechanisms linked to pathogenesis, immune evasion and viral drug resistance. In addition,
85 viral mutation studies can be crucial for the design of new vaccines, antiviral drugs and
86 diagnostic tests. A previous study (6) based on an analysis of 103 genomes of SARS-CoV-
87 2 indicates that this virus has evolved into two main types. Type L being more widespread
88 than type S, and type S representing the ancestral version. In addition, another study (7)
89 conducted on 32 genomes of strains sampled from China, Thailand and the United States
90 between December 24, 2019 and January 23, 2020 suggested increasing tree-like signals
91 from 0 to 8.2%, 18.2% and 25,4% over time, which may indicate an increase in the genetic
92 diversity of SARS-CoV-2 in human hosts.

93 Therefore, analyzing viral mutations and monitoring of the evolution capacity over time of
94 SARS-CoV-2 in a large population is necessary. In this study, we characterized the genetic

95 variants in 3067 complete genomes of SARS-CoV-2 to assess the genetic diversity of
96 SARS-CoV-2 and to track mutations accumulation over time geographic location. On the
97 other hand, we established selective pressure analysis to predict negatively selected
98 residues which could be useful for the design of therapeutic targets. We have also created
99 a database containing the comparative genomic analysis of the SARS-CoV-2 genomes, in
100 order to facilitate comparison and research for the COVID-19 scientific community.

101 **Materials and Methods**

102 **Data collection and Variant calling analysis**

103 3067 sequences of SARS-CoV-2 were collected from the GISAID EpiCovTM (update: 02-
104 04-2020) and NCBI (update: 20-03-2020) databases. Only complete genomes were used
105 in this study. **Table S1** illustrating detailed information on the genomes downloaded.
106 Genomes were mapped to the reference sequence Wuhan-Hu-1/2019 using Minimap
107 v2.12-r847-dirty (8).The BAM files were sorted by SAMtools sort (9). The final sorted
108 BAM files were used to call the genetic variants in variant call format (VCF) by SAMtools
109 mpileup (9) and bcftools (9). The final call set of the 3067 genomes, was annotated and
110 their impact was predicted using SnpEff v4.3t (10). First, the SnpEff databases were built
111 locally using annotations of the reference genome NC_045512.2 obtained in GFF format
112 from NCBI database. Then, the SnpEff database was used to annotate SNPs and InDels
113 with putative functional effects according to the categories defined in the SnpEff manual
114 (http://snpeff.sourceforge.net/SnpEff_manual.html).

115 **Phylogenetic analysis and geo-distribution**

116 The downloaded full-length genome sequences of coronaviruses isolated from different
117 hosts from public databases were subjected to multiple sequence alignments using Muscle
118 v 3.8 (11). Maximum-likelihood phylogenetic trees with 1000 bootstrap replicates were
119 constructed using RaxML v 8.2.12 (39), Tree was done using figtree v 1.4.4(12)

120 **Selective pressure and modelling**

121 We used Hyphy v2.5.8 (13) to estimate synonymous and non-synonymous ratio dN / dS
122 (ω). Two datasets of 191 and 433 for orf1ab and genes respectively were retrieved from
123 Genbank (<http://www.ncbi.nlm.nih.gov/genbank/>). After deletion of duplicated and
124 cleaning the sequences, only 92 and 35 for orf1ab and spike proteins, respectively, were

125 used for the analysis. The selected nucleotide sequences of each dataset were aligned using
126 Clustalw codon-by-codon and the phylogenetic tree was obtained using ML (maximum
127 likelihood) available in MEGA X (14). For this analysis, four Hyphy's methods were used
128 to study site-specific selection: SLAC (Single-Likelihood Ancestor Counting (15), FEL
129 (Fixed Effects Likelihood) (15) ,FUBAR (Fast, Unconstrained Bayesian AppRoximation)
130 (16) and MEME (Mixed Effects Model of Evolution) (17). For all the methods, values
131 supplied by default were used for statistical confirmation and the overall ω value was
132 calculated according to ML trees under General Time Reversible Model (GTR model). The
133 CI- TASSER generated models (<https://zhanglab.cccb.med.umich.edu/COVID-19/>) of
134 ORF1ab nonstructural proteins (NSP) 3,4,6,12,13,14 and 16 were used to highlight the
135 sites under selective pressure on the protein, due to the lack of their experimental structures
136 and the absence of suitable templates for homology modelling. On the other hand, the cryo-
137 EM structure with PDB id 6VSB was used as a model for the gene S in its prefusion
138 conformation. Structure visualization and image rendering were performed in PyMOL 2.3
139 (Schrodinger LLC).

140 **Pangenome construction**

141 115 proteomes of the genus *Betacorononavirus* were obtained from the NCBI database
142 (update: 20-03-2020), of which 83 genomes belonged to the SARS-CoV-2 species and the
143 rest distributed to other species of the same genus publicly available. These proteomes were
144 used for the construction of pangenome at the inter-specific scale of *Betacoronavirus* and
145 intra-genomic of SARS-CoV-2. The strategy of best reciprocal BLAST results (18) was
146 implemented to identify all of the orthologous genes using Proteinortho v6.0b (19).
147 Proteins with an identity above 60% and sequence coverage above 75% with an e-value
148 threshold below 1e-5 were used to be considered as significant hits.

149 **Results**

150 **SARS-CoV-2 genomes used in this study**

151 In this study, we used 3,067 SARS-CoV2 complete genomes collected from GISAID
152 EpiCovTM (update: 02-04-2020) and NCBI (update: 20-03-2020) databases. These strains
153 were isolated from 59 countries (**Fig 1A**). The most represented origin was American
154 strains with 783 (25.53%), followed by strains from England, Iceland, and China with 407

155 (13.27%), 343 (11.18%), 329 (10.73%), respectively. The date of isolation was during the
156 first three months after the appearance of the SARS-CoV-2 virus, from December 24, 2019,
157 to March 25, 2020 (**Fig 1B**). Likewise, about two-thirds of these strains collected in this
158 work were isolated during March.

159 **Allele frequencies revealed a diversity of genetic variants in six SARS-CoV-2 genes**

160 To study and follow the appearance and accumulation of mutations, we traced the profiles
161 of non-synonymous mutations, and we compared their frequency in the studied population.
162 Remarkably, compared to the reference sequence Wuhan-Hu-1/2019, a total of 716
163 mutations were identified, including 457 (64%) non-synonymous and 188 (26%)
164 synonymous mutations. The rest (10%) distributed to the intergenic regions. Focusing on
165 non-synonymous mutations, the analysis of the frequencies of mutated alleles revealed the
166 presence of 39 mutations with a prevalence greater than 0.006 (0.06% of the population),
167 which corresponds to at least 20 / 3,067 SARS-CoV-2 genomes (**Fig 2**).

168 These recurring mutations were distributed in six genes with variable frequencies, of which
169 the gene coding for replicase polyprotein (ORF1ab), spike protein, membrane
170 glycoprotein, nucleocapsid phosphoprotein, ORF3a, and ORF8. Overall, ORF1ab harbored
171 more non-synonymous mutations compared to the other five genes with 22 mutations,
172 including three mutations located in NSP12-RNA-dependent RNA polymerase (M4555T,
173 T4847I and T5020I), three in NSP13-helicase (V5661A, P5703L and M5865V), two in
174 NSP5-main proteinase (G3278S and K3353R), two in NSP15-EndoRNase (I6525T,
175 Ter6668W), two in NSP3-multi domains (A876T and T1246I), one in NSP14-exonuclease
176 (S5932F) and one in NSP4-transmembrane domain 2 (F3071Y). Likewise, spike protein
177 harbored three frequent mutations, including V483A in receptor-binding domain (RBD).
178 The rest of the mutations were found in nucleocapsid phosphoprotein (S193I, S194L,
179 S197L, S202N, R203K and G204R), ORF3a (S193I, S194L, S197L, S202N, R203K and
180 G204R), membrane glycoprotein (D3G and T175M) and ORF8 (V62L and L84S).

181 **Identification of ten hyper-variable genomic hotspot in SARS-CoV-2 genomes**

182 Interestingly, among all recurrent mutations, ten were found as hotspot mutations with a
183 frequency greater than 0.10 in this study population (**Fig 2**). The most represented was
184 D614G mutation at spike protein with 43.46% (n = 1.333) of the genomes, the second was

185 L84S at ORF8 found in 23.21% (n = 712). Thus, the gene coding for orf1ab had four
186 mutations hotspots, including S5932F of NSP14-exonuclease, M5865V of NSP13-helicase
187 L3606F of NSP6-transmembrane domain and T265I of NSP2 found with 17.02%, 16.56%,
188 14.38% and 10.66% of the total genomes, respectively. For the four other hotspot mutations
189 were distributed in ORF3a (Q57H and G251V) and nucleocapsid phosphoprotein (R203K
190 and G204R).

191 **Geographical distribution and origin of mutations worldwide**

192 Out of 3067 genomes, only 105 were found to be wild type and were particularly of Chinese
193 origin. However, mutant strains were dispersed in different countries and represented up
194 to 2962 strains with different genotype profiles. We performed a geo-referencing mutation
195 analysis to identify region-specific loci. Remarkably, USA was the country with the highest
196 number of mutations, with 316 (44% of the total number of mutations), including 173
197 (24%) singleton mutation (specific to USA genomes). While the Chinese genomes
198 containing 22% of the total number of mutations, followed by France and New Zealand
199 with 4% and 2%, respectively. It is interesting to note that among the 59 countries, 26
200 harbored singleton mutations. **Table S2** illustrates the detailed singleton mutations found
201 in these countries. The majority of the genomes analyzed carried more than one mutation.
202 However, among the recurrent non-synonymous, synonymous and intergenic mutations
203 (**Fig 3**). We found G251V (in ORF3a), L84S (in ORF8) and S5932F (in ORF1ab) present
204 on all continents except Africa and Austria (**Fig 4**). While F924F, L4715L (in orf1ab),
205 D614G (in spike) and an intergenic variant at position 241 appeared in all strains except
206 those from Asia. In Algeria, the genomes harbored mutations very similar to those in
207 Europe, including two recurrent mutations T265I and Q57H of the ORF3a. Likewise, the
208 European and Dutch genomes also shared ten recurrent mutations. On the other hand,
209 continent-specific mutations have also been observed, for example in America, we found
210 seven mutations shared in almost all genomes. In addition, two mutations at positions
211 28117 and 28144 were shared by the Asian genomes, while four different positions 1059,
212 14408, 23403, 25563 and 1397, 11083, 28674, 29742 were shared by African and
213 Australian genomes (Supplementary material). The majority of these mutations are
214 considered to be transition mutations with a high ratio of A substituted by G. The genome
215 variability was more visible in Australia, New Zealand and America than in the rest of the

216 world.

217 **Evolution of mutations over time**

218 We selected the genomes of the SARS-CoV-2 virus during the first three months after the
219 appearance of this virus (December 24 to March 25). We have noticed that the mutations
220 have accumulated at a relatively constant rate (**Fig 5**). The strains selected at the end of
221 March showed a slight increase in the accumulation of mutations with an average of 11.34
222 mutations per genome, compared to the gnomes of February, December and January with
223 an average number of mutations of 9.26, 10.59 10.34 respectively. The linear curve in
224 **Figure 5** suggests a continuous accumulation of SNPs in the SARS-CoV-2 genomes in the
225 coming months. This pointed out that many countries had multiple entries for this virus
226 that could be claimed. Thus in the deduced network demonstrated transmission routes in
227 different countries.

228 The study of the accumulation of mutations over time showed a higher number of
229 mutations in the middle of the outbreak (end of January). At the same time, an increase in
230 the number of mutations in early April was also observed. The first mutations to appear
231 were mainly located in the intergenic region linked to the nucleocapsid phosphoprotein and
232 the orf8 protein. The T265I, D614G and L84S hotspot mutations located in orf1ab and
233 Spike proteins respectively were introduced into the virus for the first time in late February.

234 **Phylogeographical analysis of SARS-CoV-2 genomes**

235 The phylogenetic tree based on the whole genome alignment showed the presence of 3
236 different clades (**Fig S1**) and demonstrate that SARS-CoV-2 is wildly disseminated across
237 distinct geographical location. The results showed that several strains are closely related
238 even though they belong to different countries. Which indicate likely transfer events and
239 identify routes for geographical dissemination. For phylogenetic tree
240 (<http://moroccangenomes.ma/covid/>) showed multiple introduction dates of the virus
241 inside the USA with the first haplotype introduced related to the second epidemic wave in
242 china.

243 **Selective pressure analysis**

244 Selective pressure on ORF1ab, gene harbored a high rate of mutations and on the Spike
245 gene, indicated a single alignment-wide ω ratio of 0.571391 and 0.75951 for spike and

246 or1ab, respectively. Most sites for both genes had $\omega < 1$ values, indicating purifying
247 selection. We estimated eight sites under negative selection pressure (696, 1171, 2923,
248 3003, 3715, 5221, 5704 and 6267) and three sites under positive selection pressure (1473,
249 2244 and 3090) in ORF1ab. For spike, we found seven sites under negative selection
250 pressure (215, 474, 541, 809, 820, 921 and 1044), while only site 5 was found under
251 negative selection pressure (**Table 1**).

252 The modelling results of ORF1ab showed that the sites with positive selections were
253 distributed in NSP3 and NSP4. While the negatively selected codons were located in NSP3,
254 NSP4, NSP6, NSP12, NSP13, NSP14 and NSP16 (**Fig 6**). Thus, only one negatively
255 selected amino acid residue was observed on the receptor binding domain, suggesting that
256 there was no strong selective pressure in the region (**Fig 7**).

257 **Inter and intra-specific pan-genome analysis**

258 In order to highlight the structural proteins shared at the inter-specific scale between the
259 isolates of the genus *Betacoronavirus*, thus at the intra-genomic scale of SARS-CoV-2, we
260 have constructed a pan-genome by clustering the sets of proteins encoded in 115 genomes
261 available publicly in NCBI (update: 20-03-2020), including 83 genomes of SARS-CoV-2
262 and the rest distributed to other species of the same genus. Overall, a total of 1,190 proteins
263 were grouped into a pangenome of 94 orthologous cluster proteins, of which ten proteins
264 cluster were shared between SARS-CoV-2 and only three species of the genus
265 *Betacoronavirus* (BatCoV RaTG13, SARS-CoV and Bat Hp-betacoronavirus/
266 Zhejiang2013). Of these, BatCoV RaTG13 had more orthologous proteins shared with
267 SARS-CoV-2, followed by SARS-CoV with ten and nine orthologous proteins,
268 respectively (**Fig 8A**).

269 It is interesting to note that among all the strains used of *BetaCoronavirus*, the ORF8
270 protein was found in orthology only between SARS-RATG13 and SARS-CoV-2. In
271 addition, the ORF10 protein was found as a singleton for SARS-CoV-2. While, the analysis
272 of the pangenome at the intra-genomic scale of 83 isolates of SARS-CoV-2 (**Fig 8B**),
273 showed that ORF7b and ORF10 were two accessory proteins (proteins variable) in SARS-
274 CoV-2 genomes, while the other proteins belonged to the core proteins of SARS-CoV-2
275 (conserved in all genomes).

276 **Discussion**

277 The rate of mutations results in viral evolution and variability in the genome, thus allowing
278 viruses to escape host immunity, as well as drugs (20). Initial published data suggests that
279 SARS-CoV-2 is genetically stable (21) which may increase the effectiveness of vaccines
280 under development. The study on the genomic variation of SARS- CoV- 2 is very
281 important for the investigation of pathogenesis, disease course, prevention, and treatment
282 of SARS- CoV- 2 infection. In this study, we characterized the genetic variations in a large
283 population of SARS-CoV-2 genomes (3,067). Our results showed a diversity of mutations
284 detected with different frequencies. Overall, more than 450 non-synonymous mutations in
285 SARS-CoV-2 genomes have been identified. The orf1ab gene contains 16 non-structural
286 proteins (NSP1-NSP16) (22), and harbored more than 50 % of the frequent mutations, with
287 a high mutation number 117, 61, and 61 in the NSP3, NSP12, and NSP2 Respectively.
288 Both NSP2 and NSP3 were reported to be essential for correcting virus replication errors
289 (23). On the other, hand recent studies have suggested that mutations falling in the
290 endosome- associated- protein- like domain of the NSP2 protein, could explain why this
291 virus is more contagious than SARS (24). The Replication enzymes NSP12 to NSP16 have
292 been reported as antiviral targets for SARS-CoV (25). In the SARS-CoV-2 genomes, we
293 found that NSP12 to NSP15 harbored nine recurrent non-synonymous mutations. Among
294 them, eight identified as new mutations, including three (M4555T, T4847I, T5020I) in
295 NSP12-RNA-dependent RNA polymerase, three (V5661A, P5703L and M5865V) in
296 NSP13-Helicase, two (I6525T, Ter6668W) in NSP15-EndoRNase. However, these new
297 mutations must be taken into account when developing a vaccine using the ORF1ab protein
298 sequences as a therapeutic target.

299 A high number of mutations were identified in the spike protein, an important determinant
300 in pathogenicity that allows the virion attachment to the cell membrane by interacting with
301 the host ACE2 receptor (26). Among all the frequent mutations in this protein, the V483A
302 mutation has been identified in this receptor and found mainly in SARS-CoV-2 genomes
303 isolated from USA. This result is consistent with the study of Junxian et al. (27). Eight
304 stains from china, USA and France harbored V367F mutation previously described to
305 enhance the affinity with ACE2 receptor (27).

306 Among the 716 mutations, ten were considered hypervariable genomic hotspots with high
307 frequencies of mutated alleles such us the L3606F mutation detected in NSP6. The NSP6
308 protein works with NSP3 and NSP4 by forming double-membrane vesicles and convoluted
309 membranes involved in viral replication (28). Besides, three previously reported mutations
310 (M5865V, S5932F) and (R203K) were identified in ORF1ab and N respectively (20).
311 Moreover, intraspecies pangenome analysis of SARS-CoV-2 showed that the six of the
312 genes harboring hotspot mutations belong to the core genome.

313 Thus, under normal circumstances genomic variation increase the viruses spread and
314 pathogenicity. This happens when the virus accumulated mutation enables its virulence
315 potential (29). Genomic comparison of the studied population allowed us to gain insights
316 into virus mutations occurrence over time and within different geographic areas. In the
317 SARS-CoV virus, the SNP distribution is not random, and it is more dominant in critical
318 genes for the virus. As it was already found in many studies (20,30). Our results confirmed
319 what was previously described and elucidate the presence of numerous hotspot mutations.
320 Besides, Co-occurrence mutations were also common in different countries all along with
321 singleton mutations. In the case of the USA, the singleton mutations are driven by the single
322 group that diverged differently due to the environment, the host, and the number of
323 generations. These mutations are due to the low fidelity of reverse transcriptase (29, 31).

324 Spain, Italy, and the US contain a high number of specific mutations which may be the
325 cause of a rapid transmission, especially in the US. These specific mutations may also be
326 correlated with the critical condition in Italy and Spain.

327 In this study, we have defined 3 major clades. The clustering of these genomes revealed
328 the spread of clades to diverse geographical regions. We observed an increase of mutations
329 over time following the first dissemination event from China. Specific haplotypes were
330 also predominant to a geographical location, especially in the US. This study opens up new
331 perspectives to determine whether one of these frequent mutations will lead to biological
332 differences and their correlation with different mortality rates.

333 Among the 7 proteins of orf1ab that harbored sites under selective pressure, only NSP3
334 and NSP4 contains both residues under positive and negative selection. The modelling of
335 NSP3 domains shows that only the negative selection site 1171 (Thr- 353), was located at

336 the conserved macro domain Mac1 (previously X or ADP-ribose 1" phosphatase) (32).
337 This domain has been previously shown to be dispensable for RNA replication in the
338 context of a SARS-CoV replicon (33). However, it could counteract the host's innate
339 immune response (34). It was proposed that the 3Ecto luminal domain of NSP3 interacts
340 with the large luminal domain of NSP4 (residues 112-164) to "zip" the ER membrane and
341 induce discrete membrane formations as an important step in the generation of ER viral
342 replication organelles (35, 36). As we have shown previously by the FEL, MEME and
343 FUBAR methods, the orf1ab 2244 site coding for ILE-1426 is under positive selection
344 pressure and since it is located on the luminal 3ecto domain of the NSP3 protein, this can
345 be explained by a possible host influence on the virus in this domain. The results of selective
346 pressure analysis revealed the presence of several negatively selected residues, one of
347 which is located at the receptor-binding domain (GLN-474) and which is known by its
348 interaction with the GLN24 residue of the human ACE2 (Angiotensin-converting enzyme
349 2) receptor (37). In general, it is well-known that negatively selected sites could indicate a
350 functional constraint and could be useful for drug or vaccine target design, given their
351 conserved nature and therefore less likely to change (38).

352

353 **Conclusion**

354 The SARS-CoV-2 pandemic has caused a very large impact on health and economy
355 worldwide. Therefore, understanding genetic diversity and virus evolution become a
356 priority in the fight against the disease. Our results show several molecular facets of the
357 relevance of this virus. We identified ten non-synonymous hotspot mutations distributed
358 in six of the virus genes with high frequencies of mutated alleles. We also were able to
359 highlight an increase in mutations accumulation overtime and revealed the existence of
360 three major clades in various geographic regions. Finally, the study allowed us to identify
361 specific haplotypes by geographic location and provides a list of sites under selective
362 pressure that could serve as an interesting avenue for future studies.

363

364

365

366 **Conflict of interest**

367 The authors declare that they have no competing interests.

368

369 **Acknowledgments**

370 We sincerely thank the authors and laboratories around the world who have sequenced and
371 shared the full genome data for SARS-CoV-2 in the GISAID database. All data authors
372 can be contacted directly via www.gisaid.org

373 This work was carried out under National Funding from the Moroccan Ministry of Higher
374 Education and Scientific Research (PPR program) to AI. This work was also supported, by
375 a grant to AI from Institute of Cancer Research of the foundation Lalla Salma.

376

377 **References**

378

- 379 1. World Health Organization. Infection prevention and control during health care
380 when COVID-19 is suspected: interim guidance, 19 March 2020. World Health
381 Organization. 2020. Available from:
382 <https://apps.who.int/iris/handle/10665/331495>
- 383 2. Enjuanes LD, Cavanagh K, Holmes MMC, Lai H, Laude P, Masters P et al.
384 (2000) Coronaviridae. In: Virus taxonomy. Classification and nomenclature
385 of viruses (M. H. V. van Regenmortel, C. M. Fauquet, D. H. L. Bishop, E. B.
386 Carstens, M. K. Estes, S. M. Lemon, J. Maniloff, M. A. Mayo, D. J. McGeoch,
387 C. R. Pringle, and R. B. Wickner eds.) Academic Press, San Diego. pp 835-
388 849.
- 389 3. Yeşilbağ K, Aytoğu G. Coronavirus host divergence and novel coronavirus
390 (Sars-CoV-2) outbreak. Clinical and Experimental Ocular Trauma and
391 Infection. 2020 Apr 23;2(1):1-9.
- 392 4. Andersen KG, Rambaut A, Lipkin WI, Holmes EC, Garry RF. The proximal
393 origin of SARS-CoV-2. Nat Med. 2020;26: 450–452. DOI:10.1038/s41591-
394 020-0820-9

- 395 5. Wu F, Zhao S, Yu B, Chen YM, Wang W, Song ZG, et al. A new coronavirus
396 associated with human respiratory disease in China. *Nature*. 2020;579:265-269.
397 6. Tang X, Wu C, Li X, Song Y, Yao X, Wu X, et al. On the origin and continuing
398 evolution of SARS-CoV-2. *Natl Sci Rev*. 2020. DOI: 10.1093/nsr/nwaa036.
399 7. Li LQ, Huang T, Wang YQ, Wang ZP, Liang Y, Huang TB, et al. COVID-19
400 patients' clinical characteristics, discharge rate, and fatality rate of meta-
401 analysis. *J Med Virol*. 2020 Mar 12. Doi: 10.1002/jmv.25757.
402 8. Li H. Minimap2: pairwise alignment for nucleotide sequences. *Bioinformatics*.
403 2018;34: 3094–3100 .DOI: 10.1093/bioinformatics/bty191.
404 9. Li H, Hansaker B, Wysoker A, Fennell T, Ruan J, Homer N, et al. The Sequence
405 Alignment/Map format and SAMtools. *Bioinformatics*. 2009;25: 2078–9.
406 DOI:10.1093/bioinformatics/btp352
407 10. Cingolani P, Platts A, Wang LL, Coon M, Nguyen T, Wang L, et al. A program
408 for annotating and predicting the effects of single nucleotide polymorphisms,
409 SnpEff: SNPs in the genome of *Drosophila melanogaster* strain w1118; iso-2;
410 iso-3. *Fly (Austin)*. 2012;6: 80-92 .DOI: 10.4161/fly.1969
411 11. Edgar RC. MUSCLE: multiple sequence alignment with high accuracy and
412 high throughput. *Nucleic Acids Re*. 2004;32: 1792–1797. DOI:
413 10.1093/nar/gkh340
414 12. Rambaut, Andrew. "FigTree v1. 4." (2012).
415 13. Pond SL, Frost SD, Muse SV. HyPhy: hypothesis testing using phylogenies.
416 *Bioinformatics*. 2005;21: 676–679. DOI: 10.1093/bioinformatics/bti079
417 14. Kumar S, Stecher G, Li M, Knyaz C, Tamura. MEGA X: Molecular
418 Evolutionary Genetics Analysis across Computing Platforms. *Mol Biol Evol*.
419 2018;35: 1547-1549. DOI: 10.1093/molbev/msy096.
420 15. Pond SL, Frost SD. Not so different after all: a comparison of methods for
421 detecting amino-acid sites under selection. *Mol Biol Evol*. 2005;22: 1208-1222.
422 Doi:10.1093/molbev/msi105.
423 16. Murrell B, Moola S, Mabona A, Weighill T, Sheward D, Pond SL, et al. Fubar:
424 a fast, unconstrained Bayesian approximation for inferring selection. *Mol Biol
425 Evol*. 2013;30: 1196-1205. DOI: 10.1093/molbev/mst030

- 426 17. Murrell B, Wertheim JO, Moola S, Weighill T, Scheffler K, Pond SL. Detecting
427 Individual Sites Subject to Episodic Diversifying Selection. PLoS Genet.
428 2012;8: e1002764. Doi: 10.1371/journal.pgen.1002764
- 429 18. Jordan IK, Rogozin IB, Wolf YI, Koonin EV. Essential genes are more
430 evolutionarily conserved than are nonessential genes in bacteria. Genome Res.
431 2002;12:962–968.
- 432 19. Lechner M, Findeiß S, Steiner L, Marz M, Stadler PF, Prohaska SJ.
433 Proteinortho: detection of (Co-)orthologs in large-scale analysis. BMC
434 Bioinformatics. 2011;12:1–9. DOI:10.1186/1471-2105-12-124.
- 435 20. Pachetti M, Marini B, Benedetti F, Giudici F, Mauro E, Storici P, et al.
436 Emerging SARS-CoV-2 Mutation Hot Spots Include a Novel RNA-dependent-
437 RNA Polymerase Variant. J Transl Med. 2020;18: 179. DOI: 10.1186/s12967-
438 020-02344-6.
- 439 21. Su Y, Anderson D, Young B, Zhu F, Linster M, Kalimuddin S, et al. Discovery
440 of a 382-nt deletion during the early evolution of SARS-CoV-2. BioRxiv
441 [Preprint]. 2020 [cited 2020 March 25]. Available from:
442 <https://www.biorxiv.org/content/10.1101/2020.03.11.987222v1>
- 443 22. Khailany RA, Safdar M, Ozaslan M. Genomic characterization of a novel
444 SARS-CoV-2. Gene Rep. 2020;19:100682.
445 DOI:10.1016/j.genrep.2020.100682
- 446 23. Harcourt BH, Jukneliene D, Kanjanahaluethai A, Bechill J, Severson KM,
447 Smith CM, et al. Identification of severe acute respiratory syndrome
448 coronavirus replicase products and characterization of papain-like protease
449 activity. J Virol. 2004;78:13600-13612. DOI:10.1128/JVI.78.24.13600-
450 13612.2004
- 451 24. Angeletti S, Benvenuto D, Bianchi M, Giovanetti M, Pasquarella S, Ciccozzi
452 M.. COVID 2019: the role of the NSP2 and NSP3 in its pathogenesis. Journal
453 of Medical Virology, 2020;92:584-588.
- 454 25. Subissi L, Imbert I, Ferron F, Collet A, Coutard B, Decroly E, et al. SARS-
455 CoV ORF1b-encoded nonstructural proteins 12-16: replicative enzymes as

- 456 antiviral targets. Antiviral Res. 2014;101:122-30. DOI:
457 10.1016/j.antiviral.2013.11.006.

458 26. Hoffmann, Markus, et al. SARS-CoV-2 cell entry depends on ACE2 and
459 TMPRSS2 and is blocked by a clinically proven protease inhibitor. *Cell* (2020).

460 27. Ou J, Zhou Z, Dai R, Zhang J, Lan W, Zhao S. Emergence of RBD mutations
461 from circulating SARS-CoV-2 strains with enhanced structural stability and
462 higher human ACE2 receptor affinity of the spike protein. *bioRxiv*
463 2020.03.15.991844; doi: <https://doi.org/10.1101/2020.03.15.991844>

464 28. Angelini MM, Akhlaghpour M, Neuman BW, Buchmeier MJ. Severe acute
465 respiratory syndrome coronavirus nonstructural proteins 3, 4, and 6 induce
466 double-membrane vesicles. *mBio*. 2013 Aug 13. pii: e00524-13. DOI:
467 10.1128/mBio.00524-13.

468 29. Stern A, Yeh MT, Zinger T, et al. The Evolutionary Pathway to Virulence of
469 an RNA Virus. *Cell*. 2017;169(1):35- 46.e19. doi:10.1016/j.cell.2017.03.013.

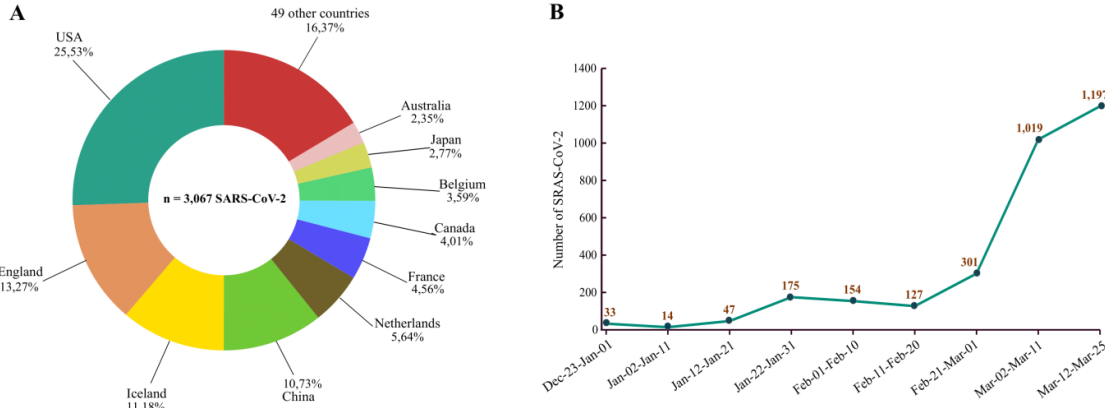
470 30. Wen F, Yu H, Guo J, Li Y, Luo K, Huang S. Identification of the hyper-variable
471 genomic hotspot for the novel coronavirus SARS-CoV-2. *J Infect*. 2020. pii:
472 S0163-4453(20)30108-0. DOI: 10.1016/j.jinf.2020.02.027.

473 31. Denison MR, Graham RL, Donaldson EF, Eckerle LD, Baric RS.
474 Coronaviruses: an RNA proofreading machine regulates replication fidelity and
475 diversity. *RNA Biol*. 2011;8: 270–279. DOI: 10.4161/rna.8.2.15013.

476 32. Neuman BW. Bioinformatics and functional analyses of coronavirus
477 nonstructural proteins involved in the formation of replicative organelles.
478 *Antiviral Res*. 2016;135: 97-107. DOI: 10.1016/j.antiviral.2016.10.005.

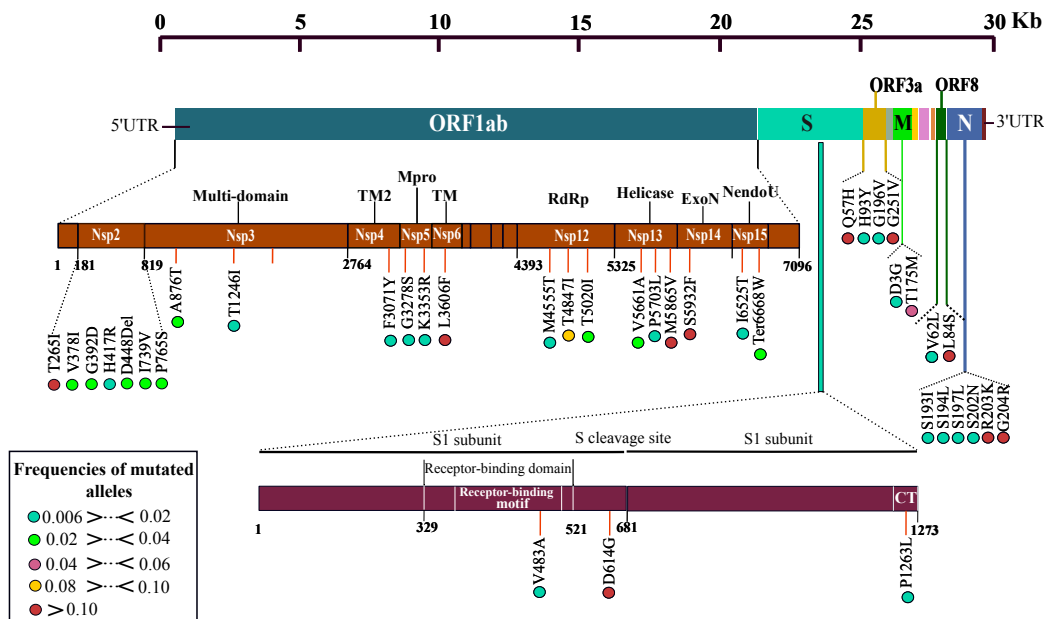
479 33. Kusov Y, Tan J, Enrique A, Luis E, Hilgenfeld R. A G-quadruplex-binding
480 macrodomain within the “SARS-unique domain” is essential for the activity of
481 the SARS-coronavirus replication-transcription complex. *Virology*. 2015;484:
482 313–322. DOI: 10.1016/j.virol.2015.06.016.

483 34. Fehr AR, Channappanavar R, Jankevicius G, Fett C, Zhao J, Athmer J. The
484 Conserved Coronavirus Macrodomain Promotes Virulence and Suppresses the
485 Innate Immune Response during Severe Acute Respiratory Syndrome



513

514 **Figure 1: Distribution of the genomes of the 3,067 genomes used in this study by**
515 **county and date of isolation. A)** The pie chart represents the percentage of genomes used in
516 this study according to their geographic origins. The colors indicate different countries. **B)** Number
517 of genomes of complete pathogens, distributed over a period of 3 months from the end of December
518 to the end of March.
519



520

521 **Figure 2: The linear diagrams represent genes distribution in the SARS-CoV-2**
522 **genome.** Diagrams in garnet and brown represent the protein subunits of ORF1ab and S
523 respectively. The presence of a mutation is represented by vertical lines. under each line, the most
524 frequent variants are annotated as the amino-acid change at that specific site, and the frequency of
525 mutations is presented by color-coded circles.
526

527

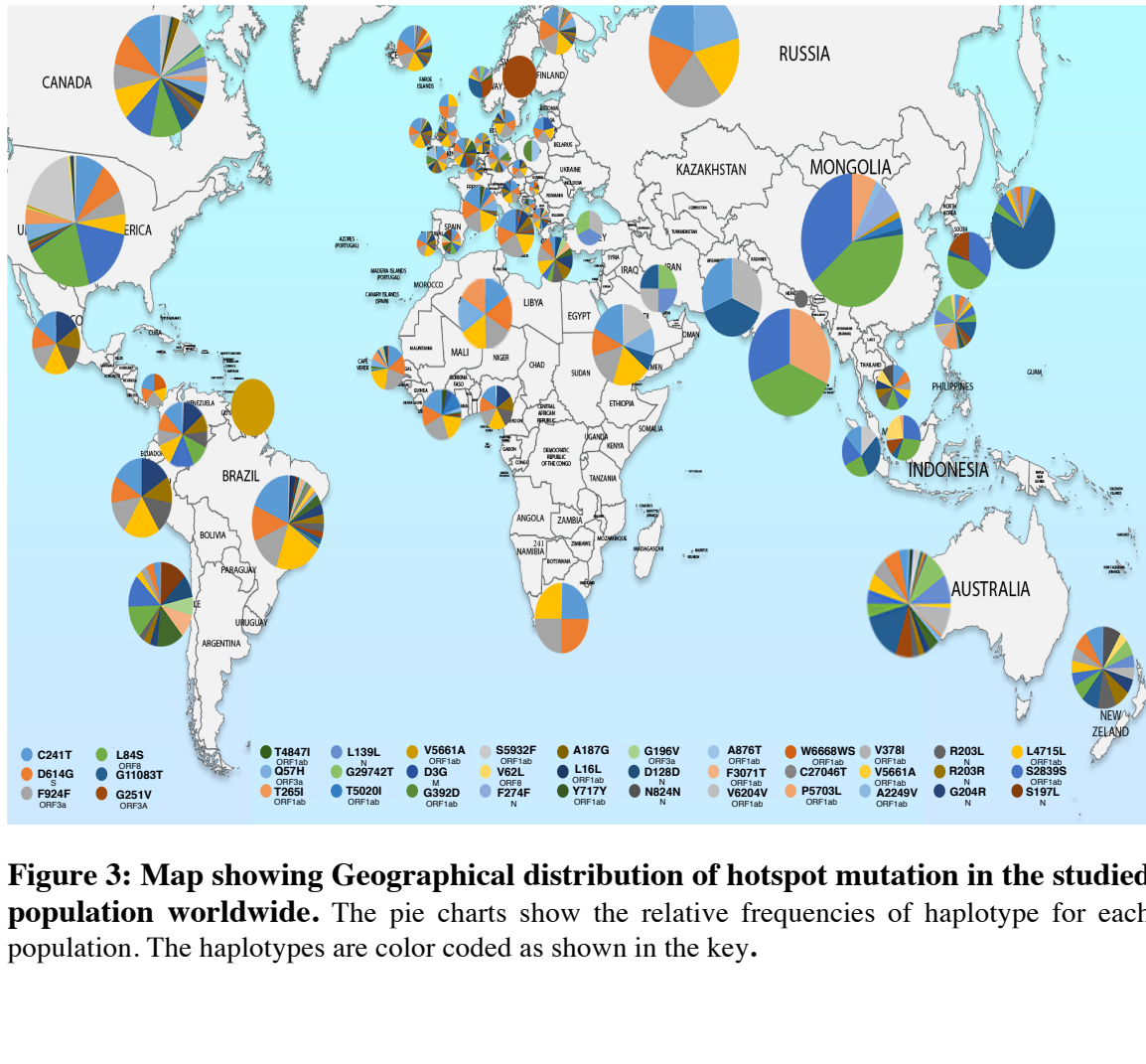
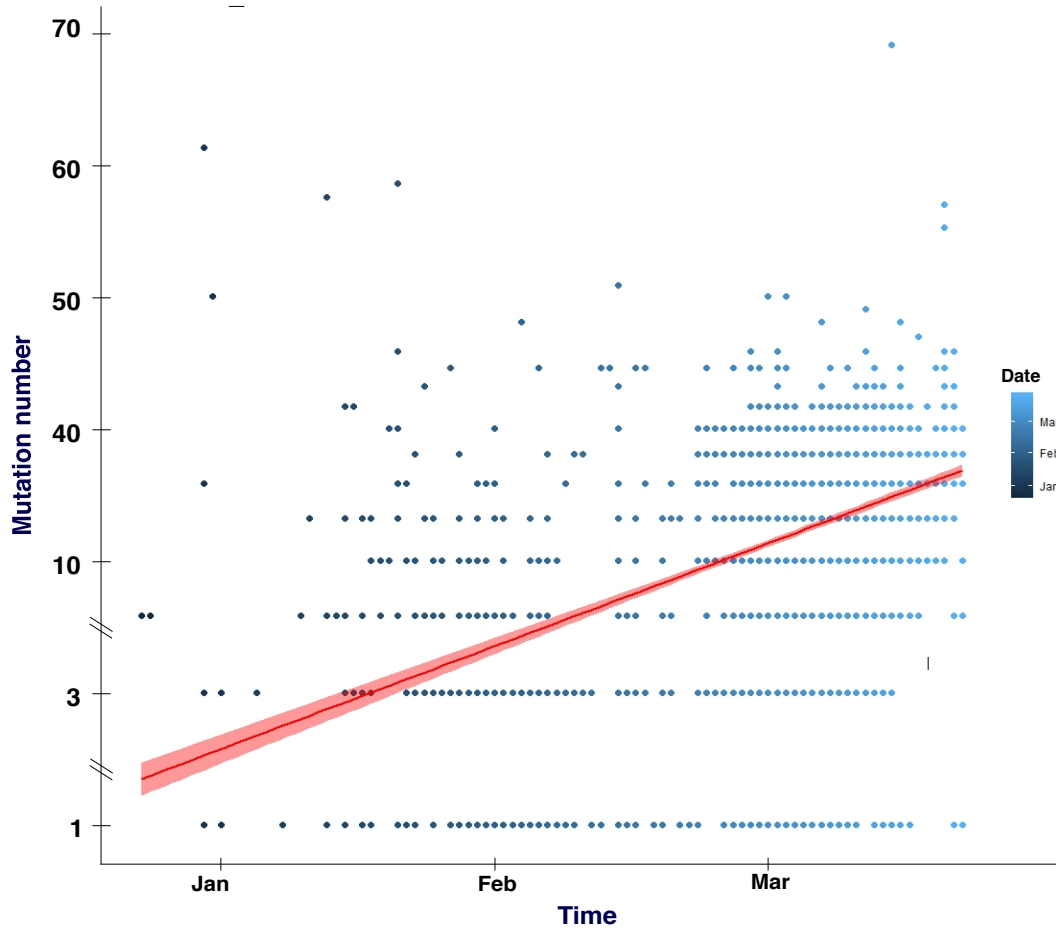


Figure 3: Map showing Geographical distribution of hotspot mutation in the studied population worldwide. The pie charts show the relative frequencies of haplotype for each population. The haplotypes are color coded as shown in the key.

546



547

Figure 4 : The graph represents substitutions accumulation in a three months period.

The accumulation of mutations increases linearly with time. The dots represent the number of mutations in a single genome. All substitutions were included non-synonymous, synonymous, intergenic.

552

553

554

555

556

557

558

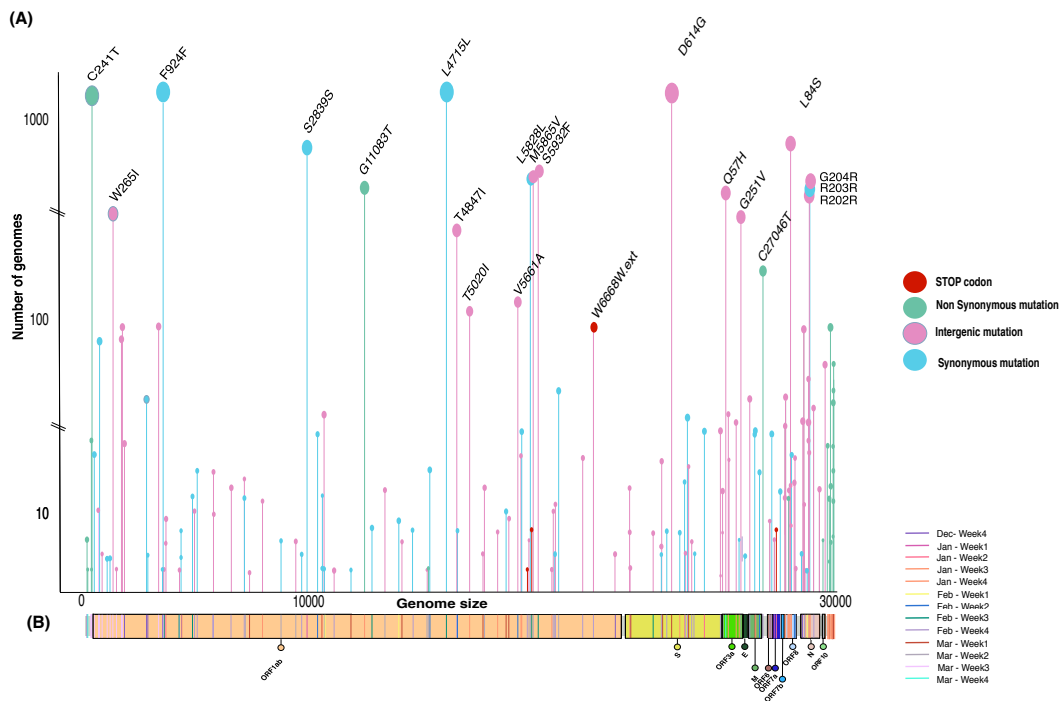
559

560

561

562

563



564

Figure 5 : Lollipop plots showing mutations distribution and frequency and time of the appearance in SARS-CoV-2 genome. A) The presence of a mutation is shown on the x-axis (lollipop), and the frequency of mutations is shown on the y-axis and correlates with the heights of the vertical lines representing each lollipop. Non-synonymous, synonymous, STOP Codon and intergenic mutations are presented as green, blue, red, and pink circles respectively. Predicted amino acid change has been represented for each hotspot mutation at the top of the circle. **B)** The diagram represents genes encoded in SARS-CoV-genome. The mutations are represented by a color-coded vertical line, each color represents a time period corresponding to the date of the first appearance of the mutation.

574

575

576

577

578

579

580

581

582

583

584

585

586

587

588

589

590

591
592
593
594
595
596
597

598
599
600
601
602
603
604
605
606
607
608
609
610
611
612

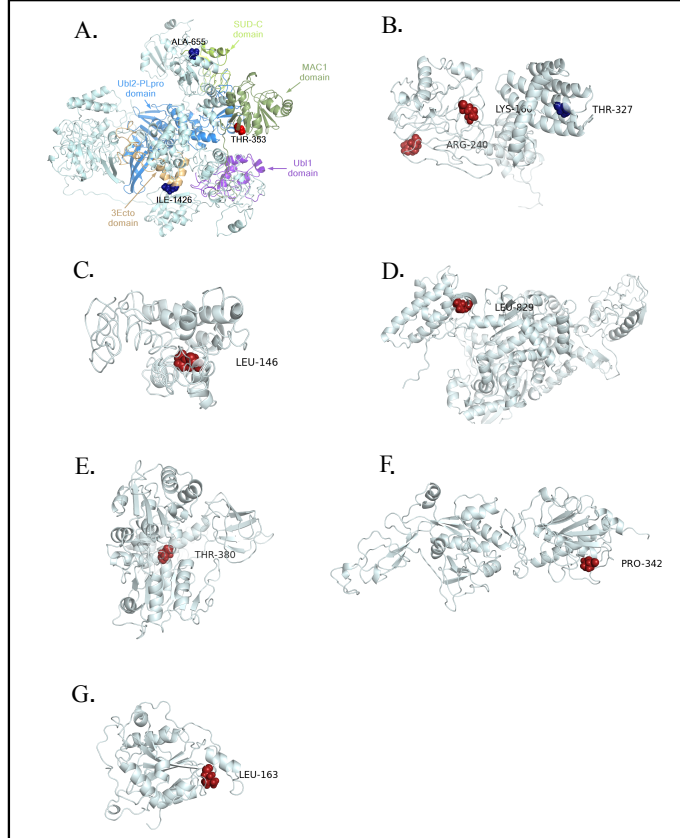
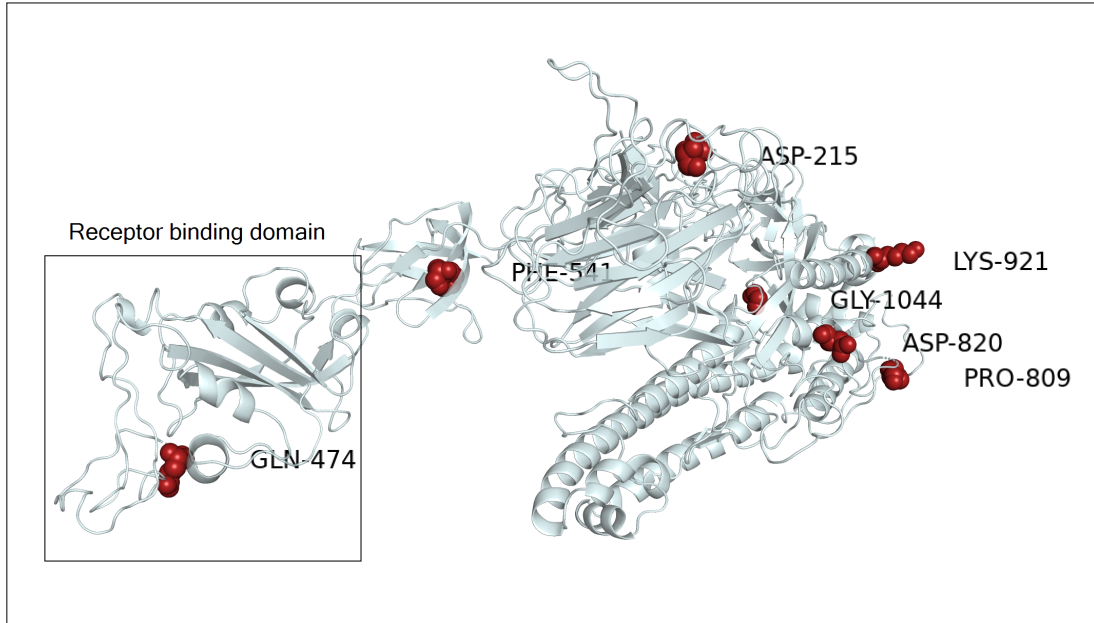


Figure6 : Structural view of selective pressure in orf1ab gene. The residue under the positive and negative selection is highlighted in blue and red respectively. The modeling of orf1ab non-structural proteins (NSP3, NSP4, NSP6, NSP12, NSP13, NSP14, and NSP16) harboring residues under pressure selection was produced using CI-TASSER. **A.** The NSP3 domains MAC1, Ubl1, Ubl2-PLpro, and SUD-C are color-coded in the 3D representation. The residues Ile-1426 and Ala-655 under negative selection are located respectively on 3Eco and SUD-C domains while Thr-353 residue under positive selection is shown on the MAC1 domain, **B.** 3D representation of the NSP4 protein, **C.** 3D representation of the NSP6 protein, **D.** 3D representation of the NSP12 protein, **E.** 3D representation of the NSP13 protein, **F.** 3D representation of the NSP14 protein, **G.** 3D representation of the NSP16 protein.

623
624
625
626
627



628

629 **Figure 7: Structural view of selective pressure in spike gene.** The negatively selected site
630 in spike protein is highlighted in red. The only amino acid residue selected negatively on the
631 receptor-binding domain corresponds to GLN-474. The cryo-EM structure with PDB id 6VSB was
632 used as a model for the gene S in its prefusion conformation.
633

634

635

636

637

638

639

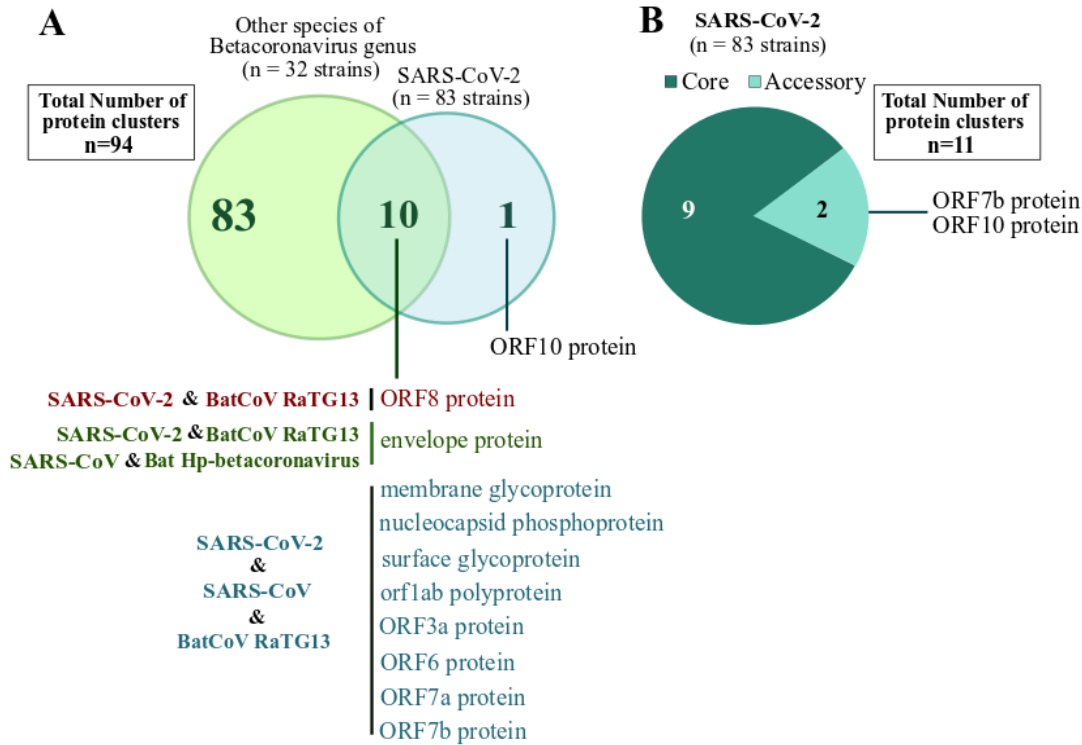
640

641

642

643

644



645
646
647
648
649
650 **Figure 8 : Pangenome analysis of 32 from different *Betacoronavirus* species and 83 of
SARS-CoV-2. (A) The Venn diagram represents the number of core, accessory, and unique
proteins inside the *Betacoronavirus* genus. (B) The pie chart illustrates the core and accessory
protein inside the SARS-CoV-2 specie.**

651

Table 1 : Selective pressure analysis on the spike and orf1ab genes of SARS-CoV-2

Genes	ω	FEL method		MEME method	SLAC method		FUBAR method	
Spike	0.571391	PS	NS	PS	PS	NS	PS	NS
		-	Codons 215, 474, 809, 820, 921,	-	-	-	Codon 5	Codons 215, 474, 541,
orf1ab	0.75951	PS	NS	PS	PS	NS	PS	NS
		Codon 2244	Codons 1171, 2923, 3003, 3715, 5221, 5704, 6267, 6961	Codon2244	-	-	Codons 1473, 2244, 3090	-

652

653